

# Enhancing sharp features by locally relaxing regularization for reconstructed images in electrical impedance tomography

Nanda V. Ranade<sup>1,3</sup>, Damayanti C. Gharpure<sup>2</sup>

1. Department of Electronic Science, Savitribai Phule Pune University, Pune, India

2. Department of Electronic Science, Savitribai Phule Pune University, Pune, India

3. E-mail any correspondence to: [nanda.ranade@gmail.com](mailto:nanda.ranade@gmail.com)

## Abstract

Image reconstruction in EIT is an inverse problem, which is ill posed and hence needs regularization. Regularization brings stability to reconstructed EIT image with respect to noise in the measured data. But this is at the cost of smoothening of sharp edges and high curvature details of shapes in the image, affecting the quality. We propose a novel iterative regularization method based on detection of probable location of the inclusion, for locally relaxing the regularization by appropriate amount, to overcome this problem. Local relaxation around inclusion allows reconstruction of its high curvature shape details or sharp features at the same time giving benefits of higher regularization in remaining areas of the image. The proposed method called DeTER is implemented using a small plug-in to EIDORS (Electrical Impedance and Diffused Optical Reconstruction Software) in a MATLAB environment. Parameters like CNR, correlation coefficients of shape descriptor functions and relative size of reconstructed targets have been computed to evaluate the effectiveness of the technique. The performance of DeTER is tested and verified on simulated data added with Gaussian noise for inclusions of different shapes. Both conducting and non-conducting inclusions are considered. The method is validated using open EIT data shared by 'Finnish inverse problem society' and also by reconstructing image of internal void of a papaya fruit from the data acquired by an EIT system developed in our laboratory. The reconstructed images corresponding to the open EIT data clearly show the shapes similar to original objects, with sharp edges and curvature details. The shapes obtained in the papaya image are shown to correspond to the actual void using shape descriptor function. The results demonstrate that the proposed method enhances the sharp features in the reconstructed image with few iterations without causing geometric distortions like smoothening or rounding of the edges.

**Keywords:** EIT, reconstruction, regularization, high curvature shape details, sharp features

## Introduction

Electrical Impedance Tomography (EIT) is an important technique for imaging internal conductivity distribution of objects from surface measurements (Barber and Brown 1984). EIT is low cost, radiation-free and noninvasive; hence extensively researched for medical imaging (Vergara *et al.* 2017). It consists of solving the reconstruction problem of finding the internal conductivity distribution from external voltage measurements. This inverse problem is ill posed (Lionheart 1990) and hence the solution is very sensitive to noise in the measurements. Surface potential measurements obtained on human subjects naturally tend to be noisy. Hence it is important to devise methods which allow true and clear images of different body parts irrespective of noise in measurements. Regularization is used to stabilize the inverse solution in presence of noise, but this is at the cost of smoothness. The sharp features of contrasts corresponding to inclusions in the original conductivity distribution appear with diffused edges in the reconstructed image. Different methods have been proposed to eliminate this effect. Some of them are use of total variation, anisotropic filters (Borsic 2010) and use of multiple regularization schemes (Bera 2011, Javaherian 2013, Kang 2017). These methods demonstrated their use for edges of rounded inclusions. Adverse effects of regularization on the

reconstruction of shapes having higher curvature and strategy or methodology to deal with the same is not reported.

Curvature of a shape refers to the rate at which the slope of tangent changes along the shape. Shapes with high curvature have sharp features as shown in Fig. 1(a). Several objects of interest in medical imaging and process tomography possess high curvature and appear as high contrast in conductivity on smooth background. Fig. 1(d) shows the anatomy of femur bone. Its ends have specific shapes, which are used for identifying anatomical landmarks (Subburaj et al. 2009). Fig.1(c) shows an MRI image of brain with the specific shape of the lateral ventricle. Such shapes could be used for image registration in multimodal imaging (Ming et al. 2007). Fig.1(b) shows the internal structure of a standard reactor used in industrial processes. High curvature details of process equipment affect the internal flow. Correct information about them allows better models to be developed. True reconstruction of shapes in (b), (c) and (d) is necessary and immensely useful, but EIT reconstruction of these sharp features would smoothen them due to regularization.

We have addressed this issue and suggested a solution to improve the image quality, by proposing a new method to locally relax regularization based on the presence of inclusion. This method is named as DeTER – Detection of Target and Edge Refinement. DeTER is implemented in open source reconstruction software EIDORS3.5 (Polydorides and Lionheart 2002). It is verified on simulated data added with Gaussian noise. It is validated using the recently shared open EIT data (Hauptman et al. 2017) acquired from tank experiments. Further it is also validated using EIT data acquired for a papaya fruit using a system developed in our laboratory, with minimum 15 dB SNR. Results show that the DeTER technique improves quality of reconstructed images and reduces the background noise.

At the end, performance of DeTER is compared with the Total Variation (TV) method, to show that DeTER generates images with similar quality in considerably less time. This clearly demonstrates the potential of DeTER for use in real life applications. Section 2 deals with the theoretical background of DeTER and Section 3 discusses the experimental plan. The rationale behind setting values of

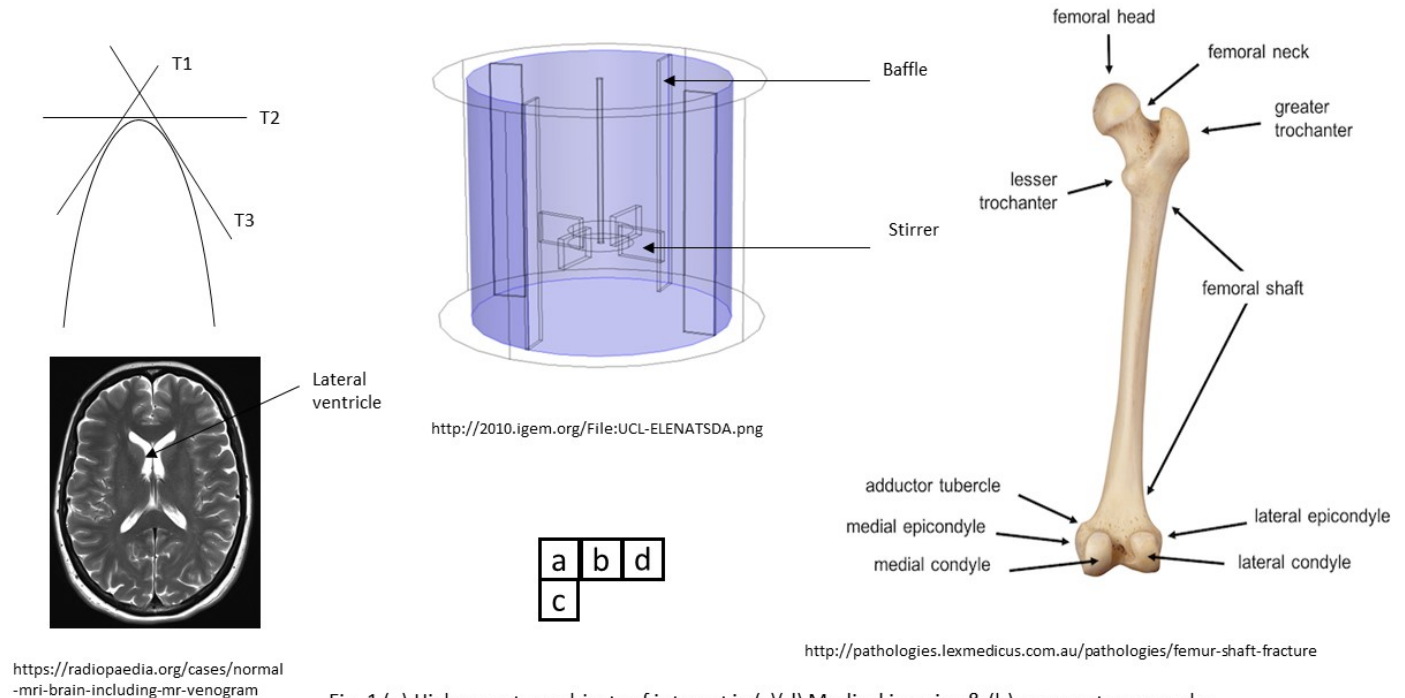


Fig. 1 (a) High curvature objects of interest in (c)(d) Medical imaging & (b) process tomography.

different variables relevant to DeTER is also discussed along with the experimental arrangement to acquire EIT data used for validation. Section 4 presents reconstructed images from simulated data, open EIT data and the data for papaya using DeTER. The enhancement in reconstructed images is quantitatively analyzed using Contrast to Noise Ratio (CNR), shape descriptor functions and corresponding correlation coefficients as well as relative size of reconstructed targets. Section 5 draws conclusions based on the results and brings out important implications of DeTER for EIT applications.

## Method

### Theoretical background of DeTER

EIT estimates internal conductivity distribution of a body. This estimation requires solution of a nonlinear ill-posed inverse problem. In EIT, the measurements carry less information of the fine details in edge shapes and this results in the regularization having a stronger impact on the properties of the reconstructed images leading to geometric distortions (Gonzalez 2017). The inverse solver 'aa\_inv\_solve' in EIDORS3.5 is based on the work of Adler

and Guardo (1996). It offers a one-step solution to the linearized inverse problem of EIT using equation 1.

$$\hat{x} = [(J'wJ + \lambda^2 R'R)^{-1} J'w] dv \quad (1)$$

$\hat{x}$  is the expected conductivity distribution,  $J$  is the jacobian,  $W$  is an inverse matrix of covariance of measurements,  $\lambda$  is the hyper parameter,  $R$  is regularization matrix and  $dv$  is the difference between two frames of measured surface potential data. The term in the square brackets is called reconstruction matrix. It is unstable in the absence of regularization and hence noise in measured data affects the reconstructed conductivity distribution. Regularization is equivalent to adding some prior information about the possible solution. EIDORS provides different types of priors. Some examples are NOSER, Tikhonov, Laplace, exponential covariance, Gaussian HPF and time smooth prior. The hyper parameter value decides the amount of regularization that is introduced as a trade-off between noise removal and accuracy. Higher value of the hyper parameter enforces strict regularization and results in a stable solution but at the cost of smoothness and loss of shape details.

Adler and Lionheart (2006) showed how to relax the regularization in case of a Tikhonov prior on specific elements by multiplying the corresponding elements of matrix  $R'R$ . They called these elements as target elements and showed that choice of these elements influences the reconstructed shape. We have used this concept to enhance sharp features in the reconstructed image, irrespective of high value of the hyper parameter. The idea is to get the location of target elements from the reconstructed images and use it iteratively to relax regularization for the next reconstruction leading to edge refinement sensitive to the shapes of the edges in the imaged domain.

The methodology of DeTER consists of three distinct steps as shown in Fig. 2. In the first iteration, reconstruction is carried out with hyper parameter set to sufficiently high value to ensure that effect of noise in the measured data on the reconstructed image is minimum. There are reported techniques to select optimum value of the hyper parameter  $\lambda$  (Graham et al. 2008). DeTER being an iterative technique does away with need for optimization of  $\lambda$  and an estimate on higher side is sufficient since the remaining two steps, ensure to bring out the shape details. The role of the hyper parameter is mainly to suppress the instability due to noise. Therefore, considering the minimum SNR of EIT system to be used, the hyper parameter could be set accordingly. It is possible to set prior information ( $R'R$ ) by using a function-call to any one of the available priors in EIDORS mentioned previously. The code for DeTER assumes a prior in the form of a diagonal matrix and hence NOSER and Tikhonov image priors are suitable. Tikhonov uses identity matrix and NOSER uses diagonal of  $J'wJ$  matrix as prior. In the first step, the prior strongly regulates amplitude of all the elements in the

reconstructed image. The target representing change from homogeneous background is reconstructed as image with positive or negative amplitude depending on whether it is more or less conducting than the background. The second step marks the target elements (region of interest) as elements having amplitude more than certain threshold containing the region of interest, as shown in Fig.2.

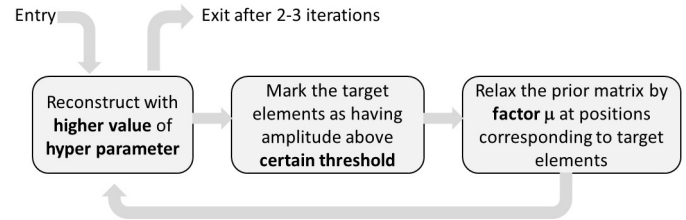


Fig.2: Flow of DeTER.

The threshold to be used is selected depending on whether the expected target is conducting or non-conducting. For conducting objects threshold is taken to be less than 1/2 of the maximum amplitude and for non-conducting objects, it is selected to be less than 1/4 of the minimum amplitude (Ranade et al. 2018). The actual value could be a heuristic choice. The choice of threshold should be such that it detects all elements belonging to an area that completely contains the object to be imaged. It is important to set the threshold appropriately to ensure that the target covers the object of interest and not a wide area around it. At the end of step 2 locations of desired elements are identified corresponding to the target.

In the third step, target is used to modify prior by multiplying the prior matrix elements by a fraction  $\mu$  at target locations. This selectively decreases the regularization only within the target area. The modified prior is used in the next iteration of reconstruction. Relaxed regularization in target area allows for sharp changes in image amplitude only in that area, enabling reconstruction of sharp features of target. At the same time, high value of hyper parameter suppresses small artifacts in the remaining area of image. This increases Contrast to Noise Ratio CNR (Bera et al. 2011) of the image. Few iterations of steps 1, 2, and 3 bring out a clear shape of the object on a homogeneous background in the reconstructed image. The important fact about the proposed method is, it derives the information about the object based on the reconstructed image and then makes required changes in the prior to relax the regularization hence it is named as 'Detection of Target and Edge Refining-DeTER regularization'. DeTER is based on difference reconstruction. Hence it is applicable in cases where interest is in finding the presence of target and not the conductivity variation within the target. It is suitable for targets having uniform conductivity giving single step change on a homogeneous background since edges are detected based on single value of threshold in step 2. The applications shown

in Fig. 1 (b, c, d) have targets of this type and DeTER is useful to enhance reconstructed images of such targets.

### Experimental plan

The theme of iterative reconstruction with modified prior proposed in the previous section is verified using a number of simulation experiments. To illustrate utility of the approach on measured data the results are validated using EIT open data. Finally, to evaluate the potential of DeTER for Non-Destructive Testing (NDT) of fruits, the methodology is applied to data collected by an EIT system developed in our laboratory (Ranade and Gharpure 2015). This section provides details of simulations carried out for verification and experiments with real data for validation.

Since the objective is to recover sharp features of inclusions, two conductivity configurations are considered. Diamond shaped target, representing convex shape and cross shaped target representing concave shape both on homogeneous background. The finite element model used for simulations has a large (3136) number of elements in order to clearly define the shapes. Fig. 3 shows the conductivity distribution for each case with uniform target conductivity equal to 0.025 S/m (i.e. nonconducting) on the background of 0.05 S/m.

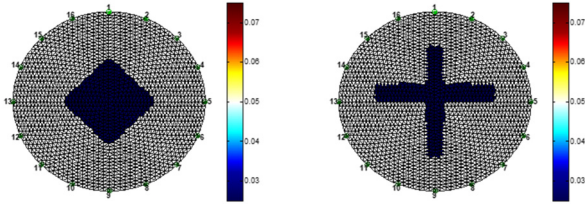


Fig.3: Conductivity distributions simulated to verify use of DeTER.

The forward problem of EIT is solved for these configurations to generate simulated data for surface potentials. Gaussian noise is added to this data to simulate realistic data from a system with SNR of 12 dB. In this paper differential reconstructions are carried out using ‘aa\_inv\_solve’, as typically used in clinical applications for stability reasons. Prior is modified as explained earlier in the second step of DeTER and plugged into the EIDORS3.5 code. Assuming hyperparameter  $\lambda$  set to one the equation 1 is modified in the target region as

$$\hat{x} = [(J'wJ + \mu R'R)^{-1}J'w]dv \quad (2)$$

Selection of hyper parameter, type of prior, threshold used for target elements and fraction  $\mu$  used to decide relaxation on regularization, play an important role in the implementation of DeTER. Reconstructions are carried out for cross shape object with different values of these variables changing them one at a time to decide the appropriate values.

Graham et al. (2008) discussed the ‘Best Res’ method to choose hyper parameter. They used real data with SNR equal to 46 dB to decide the optimum value of hyper parameter. They have shown that the hyper parameter selected using ‘Best Res’ method worked better than four other methods. We have used the hyper parameter value decided by them as our reference. The value of  $(\lambda_{Best\ Res})$  obtained from the reported graphs is found to be approximately 0.17.

Considering the value of  $\lambda$  equal to one, Equation 2 gives the solution in the target area. This means that  $\mu$  plays the role of square of hyper parameter in the target area. Hence,  $\mu$  is decided as:

$$\mu = \lambda_{Best\ Res}^2 = 0.17^2 \sim 0.03$$

EIT data having lower value of SNR (the one to be used in our work) than the one used in these experiments (46 dB) will require higher regularization. Hence  $\mu$  was set to higher approximation equal to 0.05. This value of  $\mu$  is found to result in optimum regularization in the target area.

### Image quality parameters

The nature of reconstructed images having different values of hyper parameter, threshold and type of prior is analyzed visually as well as using CNR and shape descriptor functions. CNR is defined as follows (Bera et al. 2011)

$$CNR = \frac{BC_{mean} - IC_{mean}}{\sqrt{(W_I SD_{IC}^2 + W_B SD_{BC}^2)}} \quad (3)$$

Where  $IC_{mean}$  and  $BC_{mean}$  are mean conductivities of target and background,  $SD_{IC}$  and  $SD_{BC}$  are standard deviations and  $W_I$  and  $W_B$  are fraction of total area for target and background respectively in the reconstructed image. The shape descriptor function is plotted as radial distance of point on the boundary of particular shape (target) versus the angle it makes with positive y-axis (Gonzalez 1977). Open source software ‘GeoGebra’ is used for getting the ‘r,  $\theta$ ’ values required to plot the function.

Appropriate prior and values of  $\lambda$ ,  $\mu$  are decided through simulations using cross-shaped target. The proposed reconstruction method is also verified on diamond shaped target.

EIT open data shared by the group at Kuopio University (April, 2017) is used for validation of DeTER. This data is collected on flat tank with diameter equal to 28 cm fitted with 16 steel electrodes. Electrically resistive inclusions of different shape are used on the background of saline solution with conductivity  $300 \mu S m^{-1}$ . Several data sets with different current injection patterns are made available. The photographs of the tank and targets are also available to be used for validating reconstructions. Since our interest is in enhancing sharp features, a data set corresponding to a single triangular and two circular resistive inclusions

(targets) is used. Adjacent current excitation with measurements collected on all electrodes are used for reconstruction. Both 'NOSER' and 'Tikhonov' priors are used. Validation is also done using real data collected for Papaya fruit, with DoEIT- the 16-electrode 2D EIT system developed in our laboratory. The electrode interface of DoEIT required modification as shown in Fig. 4 (a). The electrodes were chosen to be flat headed metal drawing pins. They were mounted at equal distance on an elastic band which could fit on the papaya around its center. The pins were mounted such that their flat heads touch the outer skin of the papaya and do not pierce the skin maintaining the non-invasive and non-intrusive characteristic of EIT imaging. The conductivity of material used for drawing pins is not known and was assumed to be sufficiently higher than the papaya fruit. Elastic band ensured surface contact for electrodes irrespective of uneven contours of the fruit. Two types of papaya were selected for imaging; one supposed to be with seeds (having star shaped void) and other seedless (having round void). The elastic band was mounted vertically at the center of papaya. Electrode positions were marked on the skin of papaya using a marker pen for reference. Simple wires with crocodile clips were used for connection to the electrode pins. The other ends of these wires terminated on a 'D-type' connector fitted to the system. The complete arrangement is as shown in Fig. 4 (b). Data was collected using the Sheffield protocol. Amplitude of excitation current was set to 1 mA with a frequency of 2 kHz. After collecting the data on both papaya fruits, they were cut exactly at the place where electrode belt was mounted, image was captured and the edges were extracted using image processing. This enabled the comparison of actual cross-sectional details with the reconstructed image. The analysis for papaya with star shape void is done using shape descriptor function whereas that for round void is done by calculating actual and reconstructed area of void. Finally, performance of DeTER is compared to TV method available with EIDORS which has similar objective of enhancing edges in a reconstructed image. The data acquired on papaya with star shape void is reconstructed using TV method and the resulting image is analyzed using shape descriptor function. The time required for reconstruction is compared with that for DeTER.

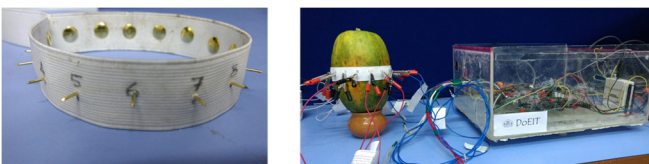


Fig.4: (a) Modified electrode interface (b) Papaya under test with electrodes attached.

#### Ethical approval

The conducted research is not related to either human or animal use.

#### Results and discussion

In this paper, a novel technique named DeTER has been proposed to enhance the sharp features in reconstructed images obtained from noisy data which demands for higher regularization. The effectiveness and use of this technique is validated based on three sets of experiments namely, simulation studies on diamond and cross shaped inclusions, open data available from Finnish institute and real data obtained in the laboratory on DoEIT. This section presents the results of various experiments carried out to verify and validate DeTER. To start with, experiments were carried out to select various parameter values in the reconstruction process. Performance of DeTER is then evaluated for the simulated data. The second part of validation presents the results and analysis of reconstructions using the Finnish open data and imaging papaya fruits using DoEIT. Initially various parameters are set based on the simulation experiments described.

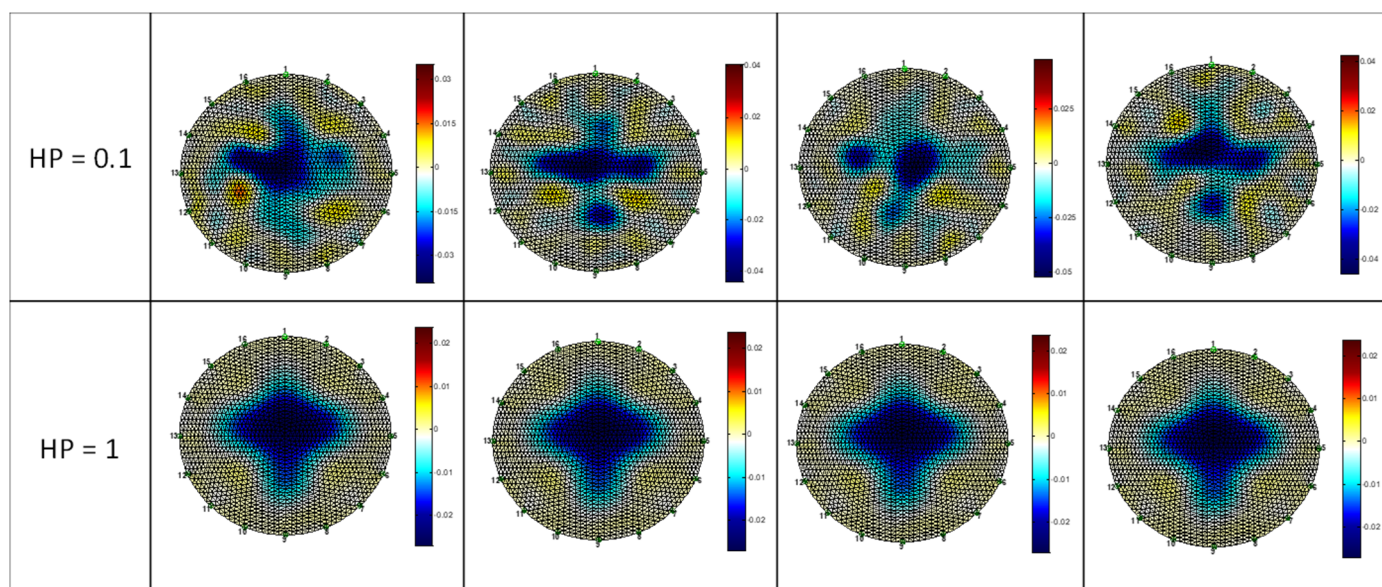
#### Setting hyper parameter

The worst-case signal to noise ratio is considered in order to set hyper parameter. The characterization of DoEIT system, reported SNR from 15 dB to 45 dB (Ranade et al. 2017). Gaussian noise equivalent to 12 dB SNR, which can be considered as the worst-case SNR, was added to simulated data. Reconstructions shown in Figure 5 of cross and diamond shaped targets, are carried out using 'aa\_inv\_solve' with NOSER prior for four different instances of noise with hyper parameter set to 1 and 0.1.

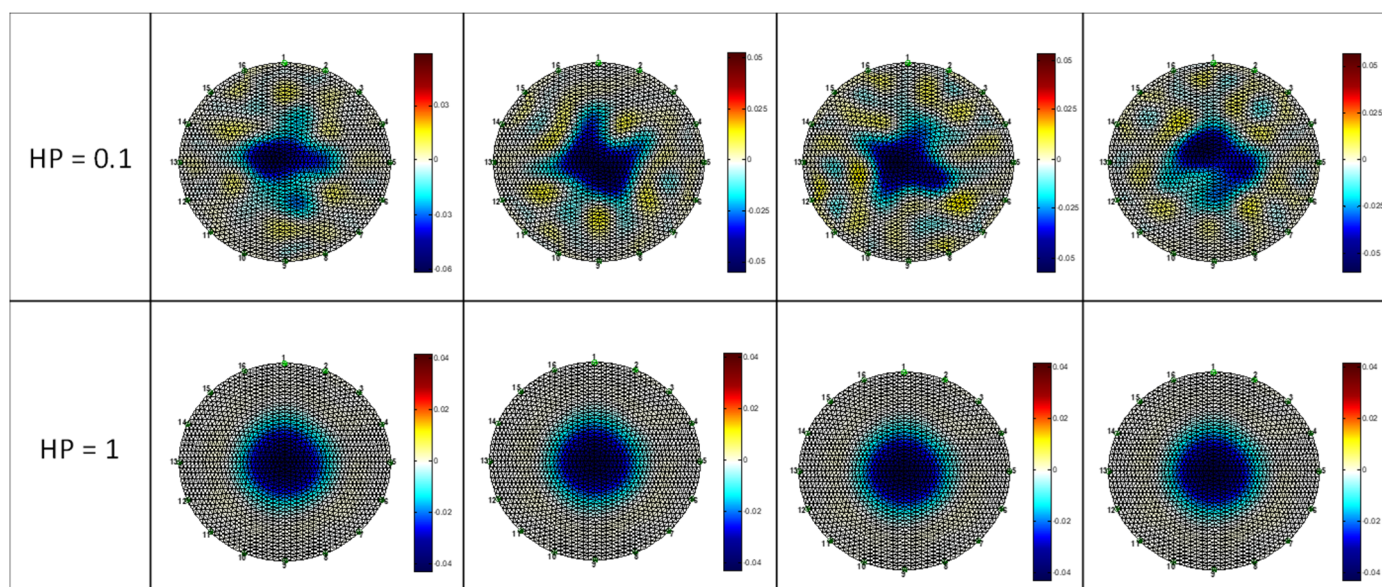
The results show that images with hyper parameter set to 0.1 are unstable and dominated with random nature of noise. The shape of reconstructed target appears different in each case. Images with hyper parameter set to 1 are stable showing the same target shape for all the 4 instances of noise. This implies that a value of the hyper parameter equal to 1 offers enough regularization for worst-case SNR. However, with the hyper parameter equal to 1, it is difficult to identify the shape of the object as a cross or a diamond.

#### Choosing type of prior

Hyper parameter is set to 1 as decided in the previous section and DeTER is used for cross shaped nonconducting target with NOSER and Tikhonov priors individually. The threshold to decide target area is set to 1/5th of the minimum amplitude since the target is non-conducting. The results with DeTER for four iterations are shown in Fig. 6. As can be seen there is no further improvement in 4'th iteration as compared to third iteration. Both the prior types give images with improved features as compared to the unmodified prior corresponding to iteration 1. The third iteration gives better image than the second. The improvement in the features is quantified by using the shape descriptor function. Fig. 7 (a) and (b) show the radial distance of points on the boundary of target from its center plotted as a function of angle for the



Reconstructions for cross shaped target



Reconstructions for diamond shaped target

Fig.5: Effect of hyper parameter in the reconstruction process HP: hyper parameter; 0.1 indicates low regularization and 1 indicates high regularization.

original cross, and the reconstructed images with and without DeTER for both Tikhonov and NOSER prior. The concave parts in the original cross are at minimum distance from the center and are represented by valleys in the plot. Reconstructed images using modified prior are decidedly closer to the original at the valley points for both Tikhonov and NOSER priors. This means DeTER is able to extract better feature details.

Fig. 7 (c) shows the correlation coefficients for shape descriptor functions of reconstructed shapes to that of the original cross. The higher value for reconstructions with DeTER points out the successful recovery of features. The CNR for reconstructed images with DeTER (6.11, 6.20) is greater than CNR without it (4.61, 4.86) for both the priors. The results also indicate that NOSER prior gives better features (corr coeff = 0.94) compared to Tikhonov prior (corr

coeff = 0.89) using DeTER. The reason for this could be traced in the value of the diagonal elements of the regularization matrix used by these priors. Tikhonov prior uses identity matrix, therefore all elements are 1. This provides uniform regularization to all finite elements. NOSER prior uses the diagonal elements of  $J'wJ$  as prior matrix (Cheney *et al.* 1990). Lower order elements of this correspond to sensitivity of measurements to interior finite elements and should therefore be smaller compared to higher order elements, which correspond to sensitivity to finite elements near the surface. As a result, NOSER prior offers less regularization to interior elements compared to elements close to the surface. The features of the cross near the center were hence clearer with NOSER prior than with Tikhonov prior and the improvement due to DeTER is clearly visible.

**Selection of threshold for deciding target elements**

As mentioned in section 2, the case of conducting and non-conducting objects needs to be considered separately for setting the threshold to detect target area. For this purpose, cross shaped targets with conductivity equal to 0.1 S/m (conducting) and 0.025 S/m (nonconducting) on the background of 0.05 S/m were considered for simulations. Two values of threshold, 1/3rd and 1/4th of the maximum image amplitude were used to detect the anomaly in case of conducting target. Similarly, two values of threshold 1/5th and 1/7th of the minimum image amplitude were used to detect the non-conducting target. The results of reconstructions are shown in Fig.8.

Image corresponding to 1/3rd threshold shows loss of connectivity in the lower part of cross. This implies that target area is unable to completely contain the object. Image corresponding 1/4th threshold clearly shows all the features of cross in the third iteration. Hence it is appropriate to set threshold equal to 1/4th of maximum for conducting objects. Similarly, image corresponding to 1/5th threshold confirms its use for non-conducting objects. Image for threshold equal

to 1/7th shows diffused edges due to use of lower value of threshold. This shows the effect of choosing threshold higher than required (1/3rd instead of 1/4th) and lower than required (1/7th instead of 1/5th). The simulation studies indicate that DeTER works successfully, both for conducting and nonconducting targets on homogeneous background. Appropriate values of different variables, are used for verifying the proposed method on a diamond shaped nonconducting object as well. The amount of noise introduced is equivalent to 12 dB SNR. The variables in reconstructions are set as:  $\lambda = 1$ , Prior type = NOSER, Threshold = 1/5th of minimum,  $\mu = 0.05$  The results for four iterations are shown in Fig.9(a). The shape descriptor for the original diamond and the reconstructed images with and without modified NOSER prior are shown in Fig. 9(b). The comparison of correlation coefficients in Fig. 9(C) clearly indicates the improvement in reconstructed image. The CNR for reconstructed image improves from 4.67 to 6.21. DeTER is successful in reconstructing features of diamond shape and provides better CNR.

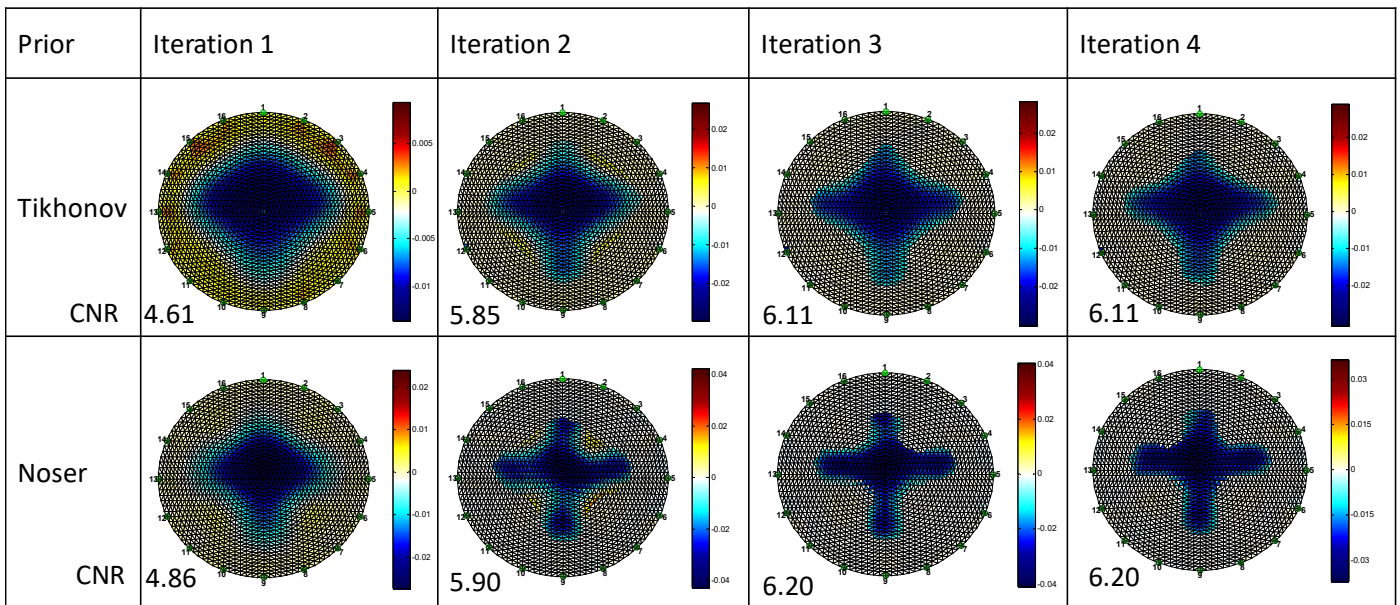


Fig.6: Effect of type of prior on reconstructed image using DeTER.

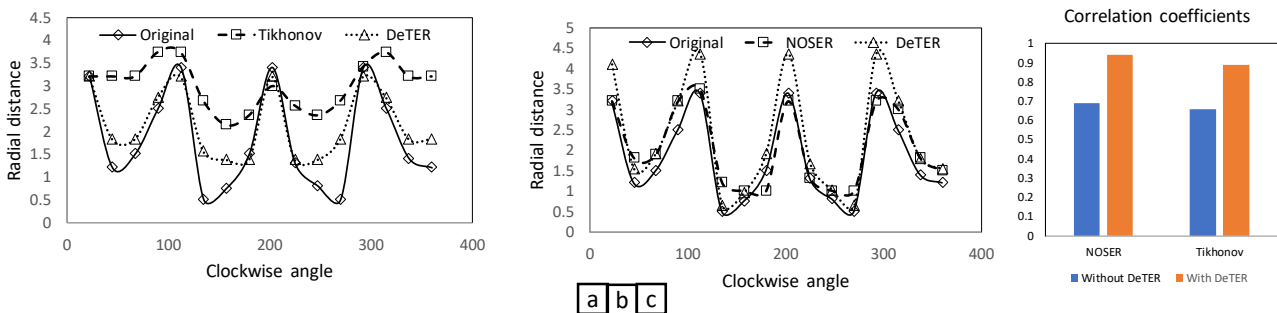


Fig.7: Plots of shape descriptor function for original and reconstructed images without and with DeTER (3rd iteration) using (a) Tikhonov and (b) NOSER prior (c) comparison of correlation coefficients for (a) and (b).

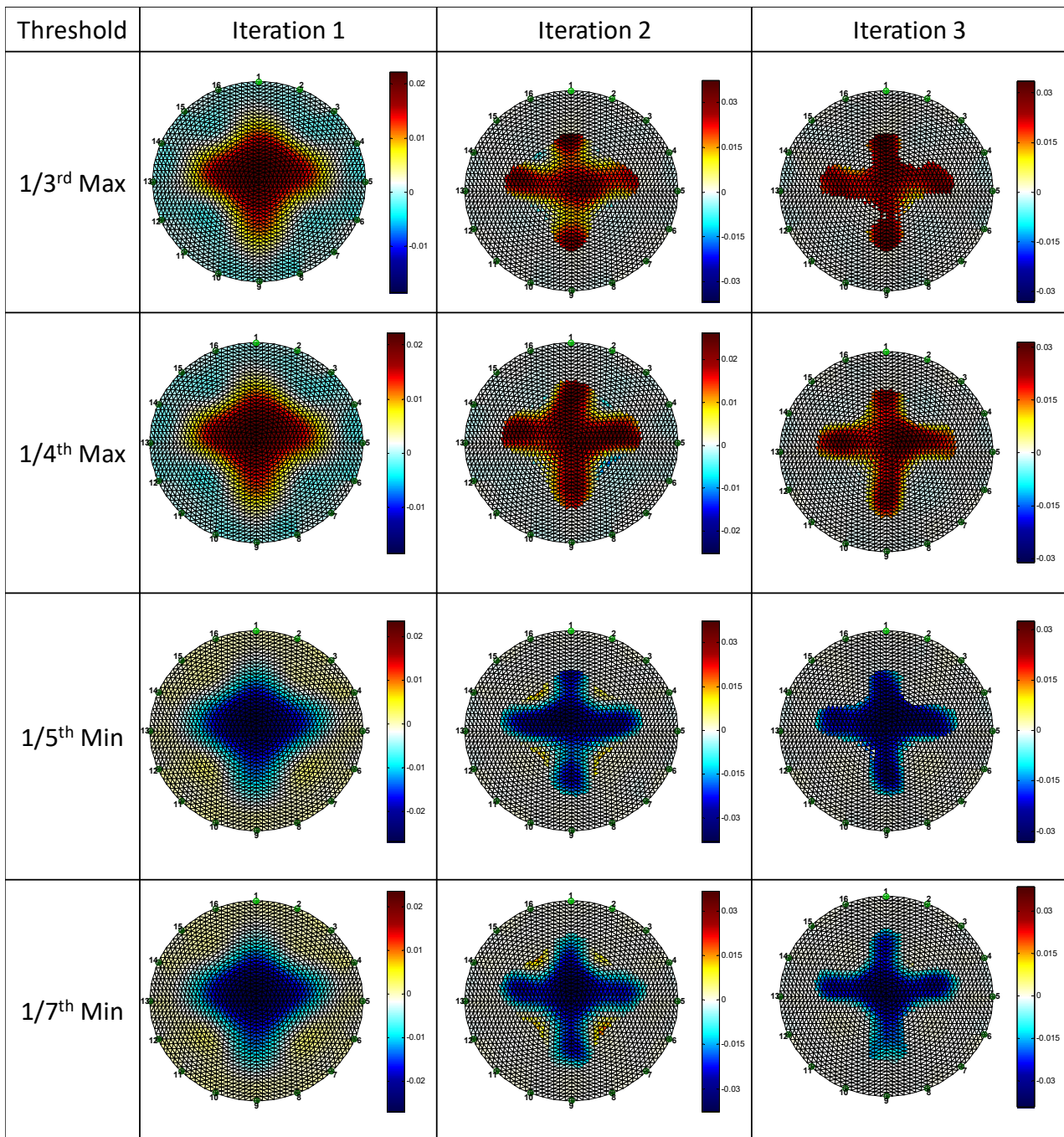


Fig.8: Effect of threshold on reconstruction of conducting and non-conducting objects.

*Validation of proposed method using real data*

To validate the utility of DeTER in the case of real data, initially open source EIT data is used. The effect of multiple inclusions (two circular and one triangular) is studied by using DeTER on Case3.3 of open data as shown in Figure 10 (a)(b)(c) along with two absolute reconstructions provided with the open data. One is with smoothness promoting prior and the other is with isotropic TV prior. Figure 10 (d)(e)(f)(g) show the reconstructed images without and with 3 iterations of DeTER using NOSER and Tikhonov priors. The reconstruction algorithms without DeTER result in smoothening of the

boundary of the triangle distorting the shape. DeTER is used with hyper parameter equal to 1, threshold equal to 1/5th of minimum and  $\mu$  equal to 0.2 for each reconstruction. It is observed that the reconstructed images with DeTER bring out essential details of the three inclusions namely lower conductivity, comparative size and shape after three iterations. The features of triangular inclusion are studied using shape descriptor functions as in case of the cross and diamond shaped targets described previously. Considering the center at the centroid of triangle, the distance of points on the sides is denoted as 'r'.



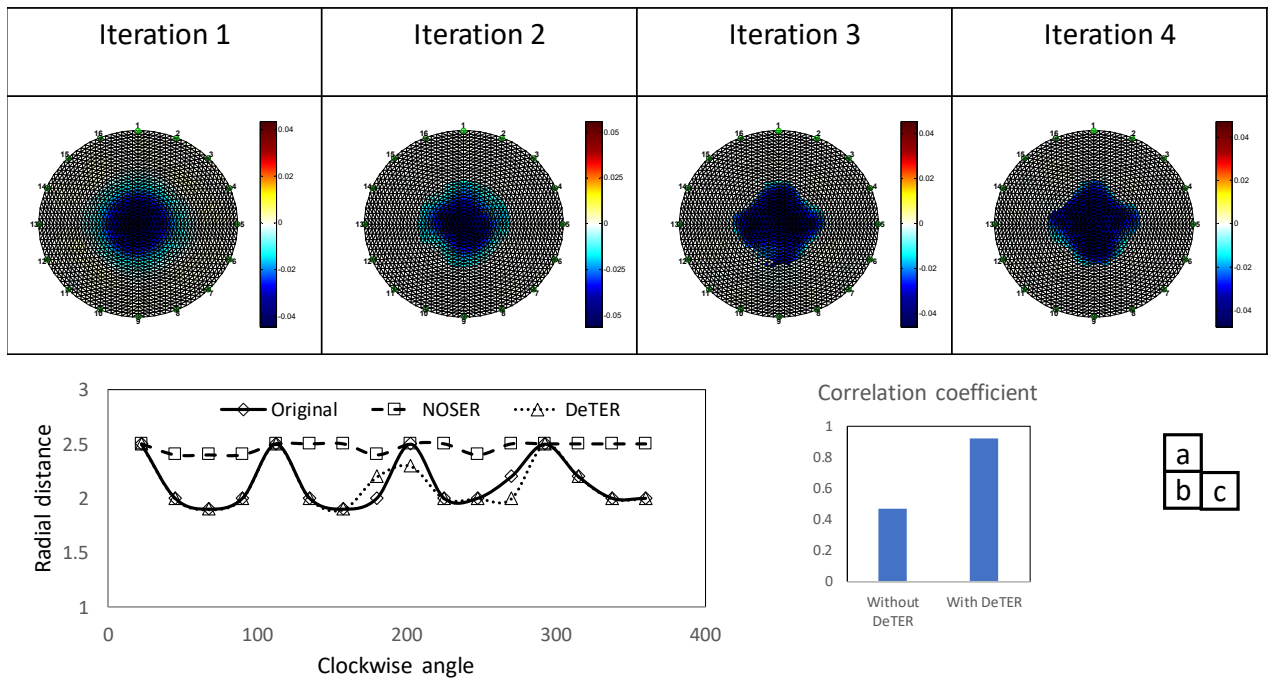


Fig.9: (a) Reconstruction of diamond shape object with DeTER using NOSER prior (b) Shape descriptor for original and reconstructed images with and without DeTER (c) Comparison of correlation coefficients.

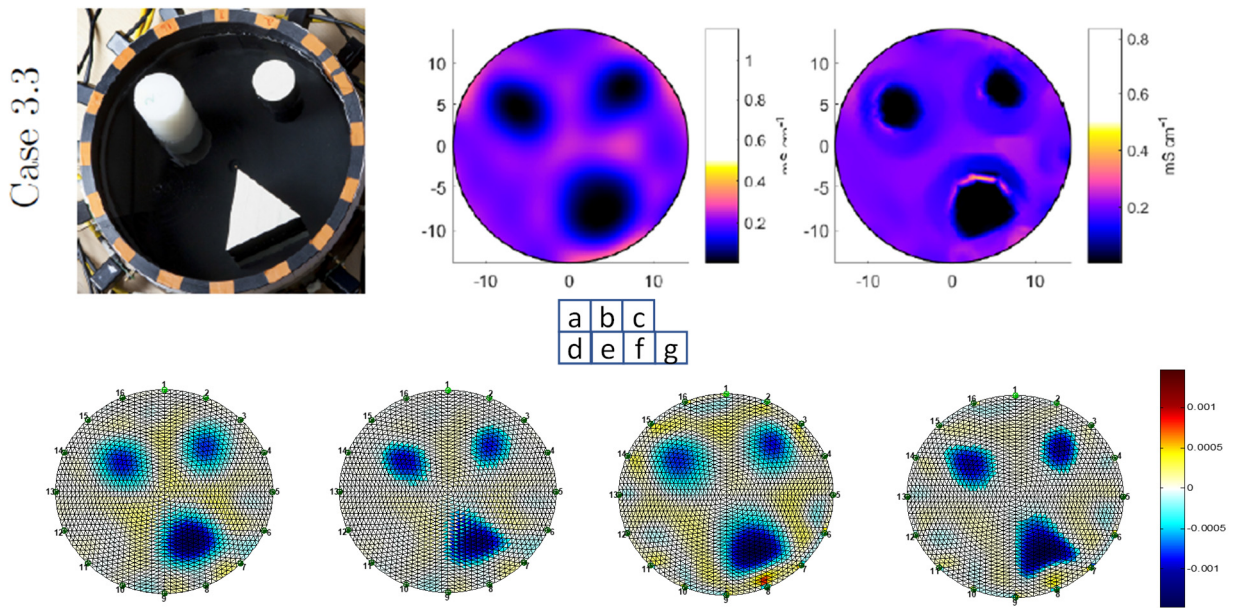


Fig.10: Reconstructions for open data. (a)(b)(c) case3.3 actual photograph with reconstructed images in open EIT data. (d)(e) Reconstructed images without and with DeTER using NOSER prior. (f)(g) Reconstructed images without and with DeTER using Tikhonov prior.

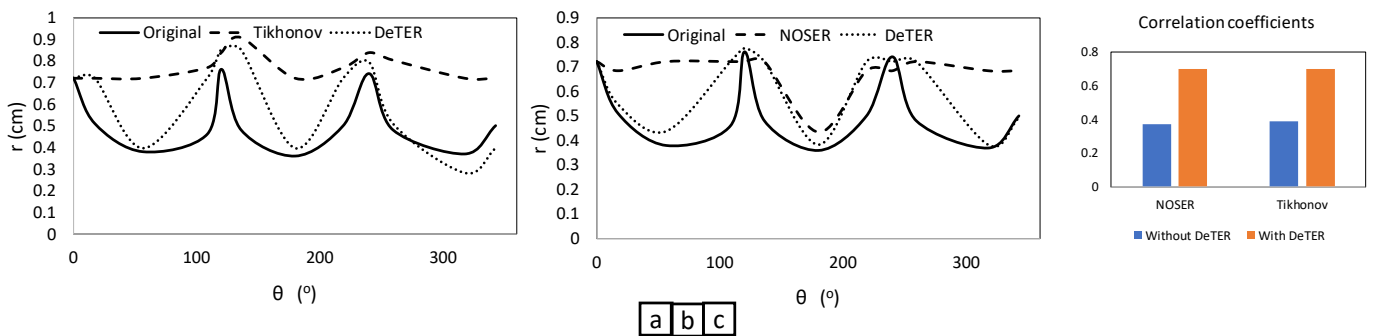





Fig.11: Shape descriptor functions for triangular target in original and reconstructed images with and without DeTER using (a) Tikhonov and (b) NOSER prior (c) comparison of correlation coefficients for (a) and (b).

Considering the vertex towards the center of the vessel as reference, angle ' $\theta$ ' is measured clockwise to plot the shape descriptor functions in the form of  $(r, \theta)$  plots. Fig. 11 (a) and (b) show the plots of the shape descriptor functions for triangular inclusion in the original image along with those for reconstructed images without and with DeTER. It is observed that the shape descriptor functions with DeTER are much closer to the original than those without DeTER for both priors. Correlation coefficients are compared in Fig. 11(c) indicating substantial improvement in features of the target. The feature details of circular targets are also studied using shape descriptor functions for all four reconstructed images in Fig. 10. The correlation coefficient with circular targets in the original image is observed to be equal to 1 for all cases. This indicates that while improving shape details of triangular inclusion, DeTER does not deteriorate the features of circular objects. It can be observed that both the reconstructions using NOSER and Tikhonov prior bring out essential details of three inclusions; lower conductivity, comparative size and shape. The features of triangular inclusion are much better compared to the two absolute reconstructions. The Tikhonov prior seems to provide continuous and clear image of inclusion compared to the NOSER prior. Further evaluation of reconstructed images is carried out by calculating percentage relative area of each reconstructed target with respect to the vessel. Since the open data does not mention the size of targets used, the relative size is derived from the photograph. The reconstructed images are binarized with a threshold value specified earlier  $-1/4$ th of minimum amplitude.

Fig.12(a) gives the comparison of relative target area expressed as percentage for all the three targets using reconstructions with and without DeTER. It is observed that DeTER with Tikhonov prior gives accurate estimate of size for all the three targets irrespective of their shape, size and position.

Target	Original	Without DeTER NOSER	With DeTER NOSER	Without DeTER Tikhonov	With DeTER Tikhonov
	5	5	5	6	5
	3	2	2	2	3
	2	1	2	2	2

a b

Fig.12: (a) Relative target area (%) for all targets in the original and reconstructed images

*The second set of real data*

The second set of real data was acquired for Papaya fruits using the DoEIT system designed in the Lab. Fig. 13 shows the reconstructed images without and with DeTER using NOSER prior along with actual photograph of horizontal section for

both papaya fruits. Papaya1 was supposed to be with seeds and papaya2 seedless. It is observed that the different nature of internal void for two papaya fruits is correctly reconstructed. The five points of the star-shape void are clearly shown in the image of papaya1. The shape analysis of papaya1 is presented in Fig. 14(a). The distance of points on the boundary of void from the center of void ( $r$ ) is plotted versus angle ( $\theta$ ) which is measured considering electrode 16 as reference.

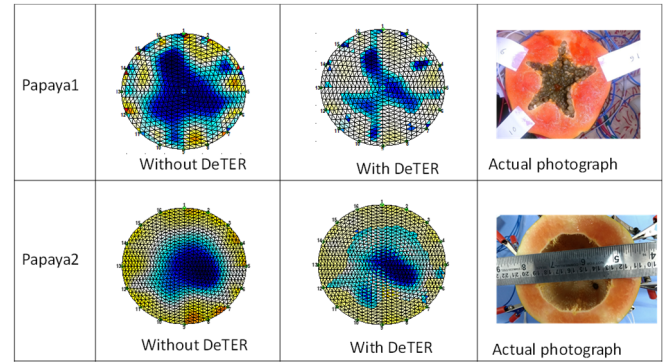


Fig.13: Reconstructed images with actual cross-sectional cuts of papaya fruits

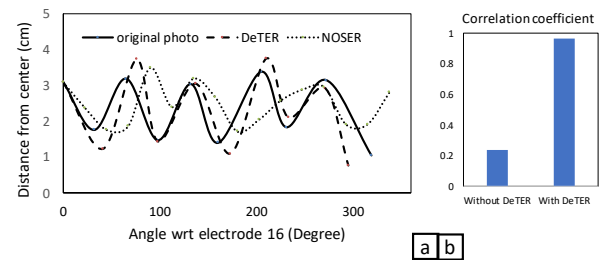


Fig.14: (a) Shape descriptor functions for void in papaya1 and its images. (b) Comparison of correlation coefficients.

The sequence followed is in the direction of increasing electrode number. The comparison of correlation coefficients for shape descriptor function of reconstructed void with the original void in Fig. 14(b) shows a clear advantage for reconstruction with DeTER. Area analysis is done for void in papaya2. Actual measured area after taking a cross cut in the fruit is  $28.27 \text{ cm}^2$ . The reconstructed area is calculated as  $31.22 \text{ cm}^2$  by first calculating relative size of the void and then multiplying it with total cross-sectional area of the papaya.

Table 1, 2 and 3 summarize the improvements in reconstructed images using DeTER by listing values of three parameters used in this paper to evaluate the images. Correlation coefficients of shape descriptor function for inclusions indicate the extent to which features of inclusions appear in the image. Relative target area is the measure of reconstructed area and CNR indicates image quality. Better

reconstructions demand higher values of correlation coefficient, CNR and same relative target area as in the original object. It is observed that reconstructions with DeTER outperform the reconstructions without DeTER in all respects for simulated, reported and the real data collected in our lab using DoEIT.

Table 1: Improvements in correlation coefficient for shape descriptor function

Parameter	Correlation coefficient for shape descriptor function				
	Simulated		Open data		DoEIT
Data	Cross	Diamond	Triangle	Circle	Papaya1
Original	1	1	1	1	1
With DeTER	0.94	0.92	0.70	1.00	0.96
Without DeTER	0.69	0.47	0.39	1.00	0.23

Table 2: Improvement in relative target area

Parameter	Relative target area (%)		
	Open data		DoEIT
Data	Triangle	Circle	Papaya2
Original	5	3	33
With DeTER	5	5	36
Without DeTER	6	2	28

Table 3: Improvement in CNR

Parameter	Contrast to noise ratio (CNR)		
	Simulated		DoEIT
Data	Cross	Diamond	Papaya1
With DeTER	6.20	6.21	6.10
Without DeTER	4.86	4.62	4.55

**Comparison with TV method**

The data acquired on Papaya1 was used for reconstruction using ‘aa\_inv\_total\_var’ routine available in EIDORS3.5. Figure 15 shows the comparison between the images reconstructed using the DeTER and TV methods along with shape descriptor functions, their correlation with actual image and the time required for reconstruction.

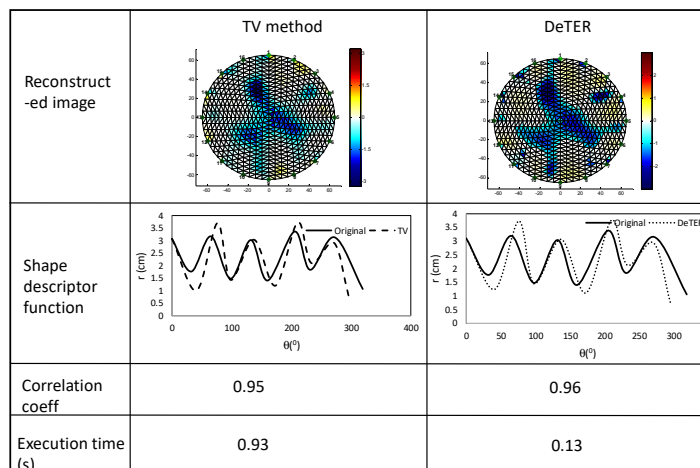


Fig.15: Comparison of DeTER with the TV method.

Both the methods offer nearly equal correlation coefficients but the time required for DeTER is nearly 1/10<sup>th</sup> of that for TV method.

**Conclusion**

In EIT, due to regularization, the fine details in edge shapes in reconstructed images are affected leading to geometric distortions (Gonzalez 2017). This paper has proposed a regularization method named DeTER, which modifies prior at selected locations for enhancing sharp features of inclusions in the reconstructed image.

Results are validated by simulations, Open EIT data and real measurements on Papaya fruit. The method has worked successfully on simulated data corrupted with noise equivalent to 12 dB SNR. The shape details of cross and diamond shaped inclusions are clearly observed after reconstruction. DeTER has performed equally well for both conducting and non-conducting inclusions on homogeneous background. CNR for all images is improved. Validation using open EIT data has shown that it successfully works in case of tank data for multiple inclusions with circular as well as triangular shapes. The method is also successful in reconstructing features of a star shaped void in papaya fruit from data acquired using DoEIT system with minimum SNR equal to 15 dB. This fact implies that DeTER could be used in practical applications of EIT requiring reconstruction of sharp features in presence of substantial noise. DeTER will be useful for all applications with targets having uniform conductivity and sharp features as mentioned in Fig.1 (b, c, d). Comparison with TV method has shown that the time required for reconstruction of desired image is 1/10<sup>th</sup> indicating improved functionality of DeTER for real time applications of EIT.

These results demonstrate that the proposed approach enhances the sharp features of an inclusion accurately without affecting smooth circular shaped edges leading to generation of more precise images. The results indicate that the visual quality of the resulting image is significantly improved and quantitative performance metrics show that the shapes of the inclusions in the reconstructed images are substantially closer to their original shapes. The improvements are verified for both simulated and real data from practical scenarios. This indicates the possibility of using EIT in different medical imaging and process tomography applications in a more meaningful way.

Future work consists of modifying DeTER to simultaneously detect conducting as well as nonconducting inclusions on homogeneous background. Using a principle similar to that of DeTER in absolute reconstruction will also be useful. Along with this it is worthwhile to explore the use of DeTER for data collected using protocols other than the Sheffield protocol used in this work.

## Conflict of interest

Authors state no conflict of interest.

## References

- Adler, A. and Guardo, R., 1996. Electrical impedance tomography: regularized imaging and contrast detection. *IEEE Transactions on Medical Imaging*, 15(2), pp.170-179.9. <https://doi.org/10.1109/42.491418>
- Adler, A. and Lionheart, W.R., 2006. Uses and abuses of EIDORS: an extensible software base for EIT. *Physiological Measurement*, 27(5), pp.S25-42. <https://doi.org/10.1088/0967-3334/27/5/s03>
- Adler, A., Arnold, J.H., Bayford, R., Borsic, A., Brown, B., Dixon, P., Faes, T.J., Frerichs, I., Gagnon, H., Gärber, Y. and Grychtol, B., 2009. GREIT: a unified approach to 2D linear EIT reconstruction of lung images. *Physiological Measurement*, 30(6), p.S35. <https://doi.org/10.1088/0967-3334/30/6/s03>
- Barber, D. C., and Brown, B. H., 1984. Applied potential tomography. *Journal of Physics E: Scientific Instruments* 17(9), p. 723
- Bera, T.K. and Nagaraju, J., 2011. Resistivity imaging of a reconfigurable phantom with circular inhomogeneities in 2D-electrical impedance tomography. *Measurement*, 44(3), pp.518-526. <https://doi.org/10.1016/j.measurement.2010.11.015>
- Bera, T.K., Biswas, S.K., Rajan, K. and Nagaraju, J., 2011. Improving Conductivity Image Quality Using Block Matrix-based Multiple Regularization (BMMR) Technique in EIT&58; A Simulation Study. *Journal of Electrical Bioimpedance*, 2(1), pp.33-47. <https://doi.org/10.5617/jeb.170>
- Breckon, W.R., 1990. Image reconstruction in electrical impedance tomography (Doctoral dissertation, Oxford Polytechnic).
- Cheney, M., Isaacson, D., Newell, J.C., Simske, S. and Goble, J., 1990. NOSER: An algorithm for solving the inverse conductivity problem. *International Journal of Imaging Systems and Technology*, 2(2), pp.66-75. <https://doi.org/10.1002/ima.1850020203>
- Cui, M., Wonka, P., Razdan, A. and Hu, J., 2007. A new image registration scheme based on curvature scale space curve matching. *The Visual Computer*, 23(8), pp.607-618. <https://doi.org/10.1007/s00371-007-0164-1>
- González, G., Kolehmainen, V. and Seppänen, A., 2017. Isotropic and anisotropic total variation regularization in electrical impedance tomography. *Computers & Mathematics with Applications*, 74(3), pp.564-576. <https://doi.org/10.1016/j.camwa.2017.05.004>
- Gonzalez, R.S. and Wintz, P., 1977. *Digital image processing*. Addison Wesley.
- Graham, B.M., 2007. Enhancements in Electrical Impedance Tomography (EIT) image reconstruction for three-dimensional lung imaging (Doctoral dissertation, University of Ottawa, Canada).
- Hauptmann, A., Kolehmainen, V., Mach, N.M., Savolainen, T., Seppänen, A. and Siltanen, S., 2017. Open 2D electrical impedance tomography data archive. arXiv preprint arXiv:1704.01178.
- Holder, D.S. ed., 2004. *Electrical impedance tomography: methods, history and applications*. CRC Press.
- Javaherian, A., Movafeghi, A. and Faghihi, R., 2013. Reducing negative effects of quadratic norm regularization on image reconstruction in electrical impedance tomography. *Applied Mathematical Modelling*, 37(8), pp.5637-5652. <https://doi.org/10.1016/j.apm.2012.11.022>
- Kang, S.I., Khambampati, A.K., Kim, B.S. and Kim, K.Y., 2017. EIT image reconstruction for two-phase flow monitoring using a sub-domain based regularization method. *Flow Measurement and Instrumentation*, 53, pp.28-38. <https://doi.org/10.1016/j.flowmeasinst.2016.06.002>
- Polydorides, N. and Lionheart, W.R., 2002. A Matlab toolkit for three-dimensional electrical impedance tomography: a contribution to the Electrical Impedance and Diffuse Optical Reconstruction Software project. *Measurement Science and Technology*, 13(12), p.1871. <https://doi.org/10.1088/0957-0233/13/12/310>
- Polydorides, N., 2002. Image reconstruction algorithms for soft field tomography (Doctoral dissertation, University of Manchester).
- Ranade, N.V. and Gharpure, D.C., 2015, March. Design and development of instrumentation for acquiring electrical impedance tomography data. In *Physics and Technology of Sensors (ISPTS), 2015 2nd IEEE International Symposium on* (pp. 97-101). <https://doi.org/10.1109/ispts.2015.7220091>
- Seagar, A.D., Barber, D.C. and Brown, B.H., 1987. Theoretical limits to sensitivity and resolution in impedance imaging. *Clinical Physics and Physiological Measurement*, 8(4A), p.13. <https://doi.org/10.1088/0143-0815/8/4a/003>
- Subburaj, K., Ravi, B. and Agarwal, M., 2009. Automated identification of anatomical landmarks on 3D bone models reconstructed from CT scan images. *Computerized Medical Imaging and Graphics*, 33(5), pp.359-368. <https://doi.org/10.1016/j.compmedimag.2009.03.001>
- Vauhkonen, M., Vadasz, D., Karjalainen, P.A., Somersalo, E. and Kaipio, J.P., 1998. Tikhonov regularization and prior information in electrical impedance tomography. *IEEE Transactions on Medical Imaging*, 17(2), pp.285-293. <https://doi.org/10.1109/42.700740>
- Vergara, S., Sbarbaro, D. and Johansen, T.A., 2017. Accurate position estimation methods based on electrical impedance tomography measurements. *Measurement Science and Technology*, 28(8), p.084003. <https://doi.org/10.1088/1361-6501/aa743f>
- Yang, Chuan Li., 2014. *Electrical impedance tomography: algorithms and applications* (Doctoral Dissertation, University of Bath, UK).